Available online at www.sciencedirect.com
ScienceDirect
Trans. Nonferrous Met. Soc. China 33(2023) 1296−1304
Transactions of Nonferrous Metals Society of China
www.tnmsc.cn

Separation of phosphorus from metallurgical-grade silicon via micro negative pressure during oxidative ladle refining

Xiao-cong DENG[1,2], Kui-xian WEI[1,2,3], Wen-hui MA[1,2,3], Qi-wei TANG[1,2], Hui ZHANG[1,2]

1. Faculty of Metallurgical and Energy Engineering, Kunming University of Science and Technology, Kunming 650093, China;
2. National Engineering Laboratory for Vacuum Metallurgy, Kunming University of Science and Technology, Kunming 650093, China;
3. Key Laboratory (MOST) of Clean Utilization in Complex Non-ferrous Metal Resources, Kunming University of Science and Technology, Kunming 650093, China

Received 16 November 2021; accepted 1 March 2022

Abstract: The stable separation of P from metallurgical-grade silicon (MG-Si) was achieved by introducing a micro negative-pressure (MNP) environment with oxidative ladle refining. The average relative removal efficiency of P was increased from −1.9428% to 21.7638% with the introduction of MNP environment. During MNP oxidative ladle refining (MNPOLR), P was not enriched in slag and instead was separated via gas phase transfer. Despite the low boiling point of P and its highly saturated vapor pressure, the volatilization of P was controlled by gas diffusion during conventional oxidative ladle refining. The continuous separation of fume via MNPOLR weakened the diffusion resistance of P in the gas phase, efficiently separating P from MG-Si. Therefore, MNPOLR is an effective P separation technique that can be widely applied.

Key words: oxidative ladle refining; micro negative pressure; separation; phosphorus; metallurgical-grade silicon

1 Introduction

Metallurgical-grade silicon (MG-Si) is the main basic material in the silicon industry chain. Phosphorus (P), a nonmetallic impurity, exerts a significant toxic effect on the production of solar-grade silicon [1] and organosilicon monomer [2]. P removal is necessary before MG-Si enters downstream operations. The only purification process that MG-Si has thus far undergone before entering downstream operations is referred to as oxidative ladle refining (OLR), which occurs during the production of MG-Si.

An electric furnace is widely regarded as the equipment primarily used for the production of MG-Si. By adding the carbonic reducing agents and silica into the furnace, crude MG-Si melt (C-MG-Si) with high impurity content can be produced. The C-MG-Si in the furnace is then put into a ladle outside the furnace for OLR, which is purified by blowing a mixture of oxygen (O_2) and air from the bottom of the ladle. A small amount of slagging agent is then occasionally added during the process. Therefore, OLR combines the characteristics of both blowing and slag refining technologies: Blowing refining is the basis of OLR. O_2 in the mixed refining medium reacts preferentially with Ca, Al, and Si in the C-MG-Si melt to form oxides (CaO, Al_2O_3, and SiO_2), which accomplishes the preliminary separation of Ca and Al [3,4]. Meanwhile, the obtained oxidation products (CaO,

Corresponding author: Kui-xian WEI, Tel: +86-13888807407, E-mail: kxwei2008@hotmail.com
DOI: 10.1016/S1003-6326(23)66183-7

Al_2O_3, and SiO_2, etc.) and slagging agents form multiple slag phases (e.g., the SiO_2−CaO−Al_2O_3 slag phase). Differences in viscosity and special interfacial tension occurred between the slag and the Si melt. With the balanced distribution of impurities in the two phases, Ca, Al, and other impurities were ultimately separated from C-MG-Si [5−7]. However, OLR is only effective for easily oxidized elements in C-MG-Si (Ca, Al, Mg, etc.) and almost ineffective for elements that are difficult to oxidize, such as P, which cannot be separated by OLR and then eventually deposited in MG-Si products [8]. This phenomenon is evidently not conducive to downstream material production, and the OLR process in MG-Si production needs to be optimized.

Currently, published research results on basic purification technologies mainly include blowing refining [9], slagging refining [10], vacuum refining [11], alloy refining [12], directional solidification [13], and acid leaching [14]. Simultaneously, the combination of two or more basic techniques is an important direction for refining technology optimization. Compared with individual methods, the combined technique provides more general adaptability to impurities and has received extensive research interest. Combined techniques, such as blowing refining + slagging refining [15,16] and alloy refining + (blowing refining [17], slagging refining [18], acid leaching [19], directional solidification [20]) have achieved higher impurity removal efficiency. Among the basic purification techniques, vacuum refining can enhance the separation of P without additives and auxiliary treatment. The advantages of vacuum refining are necessary for the optimization of OLR. To reduce the cost of obtaining vacuum conditions and adapt to the industrial production of enterprises, a new combination technology with a broad application prospect is proposed in this study. This approach introduces micro negative pressure into OLR to realize the separation of P from MG-Si.

2 Experimental

2.1 Experimental materials and processes

The OLR process is illustrated in Fig. 1(a). Crude-metallurgical grade silicon (C-MG-Si) generated in the electric furnace was placed into the ladle, and a mixture of air and oxygen (O_2) was blown in from the bottom of the ladle. MG-Si products and refining slag were obtained after refining. Figures 1(b) and 1(c) present the schematics of conventional OLR (COLR) and micro negative-pressure OLR (MNPOLR), respectively. With the MNPOLR method, fume is generated, moves toward the hood, and is collected by the cyclone dust collector. This process not only produces a cleaner production environment but also an MNP environment with pressure close to but less than the atmospheric pressure above the melt.

The concentration of P in MG-Si is a key index of product quality; thus, the separation behavior of P under with COLR and MNPOLR methods was systematically analyzed. As shown in Fig. 2, five consecutive batches of C-MG-Si, MG-Si, and refining slag from COLR and MNPOLR are obtained during the normal production of MG-Si. The mass of the samples is similar from batch to batch, remaining between 1.00 and 1.15 kg. During sampling, no slagging agent was used, and the blowing volume and time were controlled within a stable range of values. To ensure the uniformity

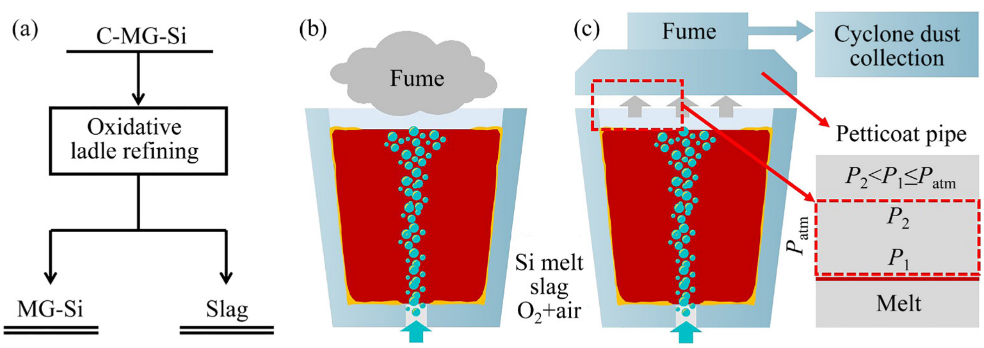

Fig. 1 Schematic of oxidative ladle refining process: (a) Flowchart of oxidative ladle refining; (b) Conventional oxidative ladle refining; (c) Micro negative-pressure oxidative ladle refining

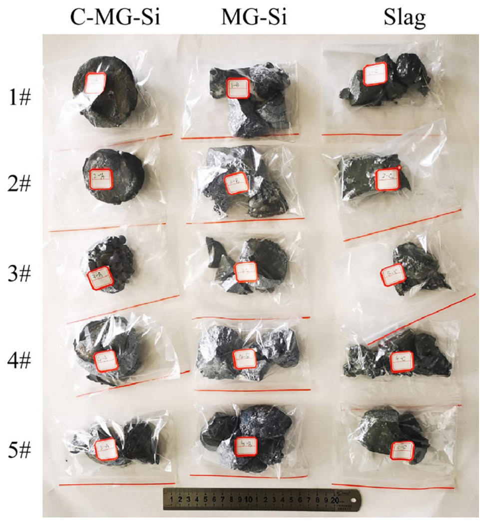

Fig. 2 Graph of sampling results

of sampling, C-MG-Si and MG-Si in liquid were directly obtained in the initial and final stages of refining by using a sampling spoon because of the nonuniformity attributed to component segregation in solid Si material.

2.2 Sample characterization and analysis

The experimental raw materials were precrushed, and the samples were ground with a ball mill. The P concentrations in C-MG-Si, MG-Si, and refining slag were quantitatively analyzed by X-ray fluorescence (XRF, ZKS100E, Japan). The P concentrations in different types (j=1, 2, 3, 4, 5) of C-MG-Si (C_j^{C}), MG-Si (C_j^{R}), and slag (C_j^{S}) were determined from the characterization results.

First, the average P concentration indices in C-MG-Si (C^{aC}) and MG-Si (C^{aR}) were calculated by comparing the characteristics of P in five types of COLR and MNPOLR materials:

$$C^{\mathrm{aC}}=\frac{1}{5}\sum_{j=1}^{5}C_j^{\mathrm{C}}=\frac{C_1^{\mathrm{C}}+C_2^{\mathrm{C}}+C_3^{\mathrm{C}}+C_4^{\mathrm{C}}+C_5^{\mathrm{C}}}{5} \tag{1}$$

$$C^{\mathrm{aR}}=\frac{1}{5}\sum_{j=1}^{5}C_j^{\mathrm{R}}=\frac{C_1^{\mathrm{R}}+C_2^{\mathrm{R}}+C_3^{\mathrm{R}}+C_4^{\mathrm{R}}+C_5^{\mathrm{R}}}{5} \tag{2}$$

Second, the relative removal efficiency (E_j) indices of P in different types of materials during COLR and MNPOLR were calculated. Meanwhile, the average relative removal efficiency (E^{a}) indices of P under the two processes were determined:

$$E_j=\frac{C_j^{\mathrm{C}}-C_j^{\mathrm{R}}}{C_j^{\mathrm{C}}}\times 100\% \tag{3}$$

$$E^{\mathrm{a}}=\frac{1}{5}\sum_{j=1}^{5}E_j=\frac{E_1+E_2+E_3+E_4+E_5}{5} \tag{4}$$

Finally, the distribution coefficient (D) of P between slag and MG-Si is an important basis for evaluating the mechanism of impurity separation, given that MG-Si and slag were obtained after refining C-MG-Si. The distribution coefficient (D_j) of P in different batches of COLR and MNPOLR materials was calculated, and the average distribution coefficient (D^{a}) of P under the two processes was also determined:

$$D_j=C_j^{\mathrm{C}}/C_j^{\mathrm{R}} \tag{5}$$

$$D^{\mathrm{a}}=\frac{1}{5}\sum_{j=1}^{5}D_j=\frac{D_1+D_2+D_3+D_4+D_5}{5} \tag{6}$$

3 Results and discussion

3.1 Effect of micro negative-pressure oxidative ladle refining on separation of P

First, the concentrations of P in C-MG-Si and MG-Si processed using COLR and MNPOLR were statistically analyzed. As shown in Fig. 3(a), the concentration of P in MG-Si was generally increased relative to that in C-MG-Si after COLR. To obtain reliable comparison results, the average concentrations of P in C-MG-Si and MG-Si during COLR were calculated based on the experiment. The results revealed that the average concentration of P in C-MG-Si before COLR was 0.0077 wt.%, and that in MG-Si after COLR was 0.0078 wt.%. This small difference implies that COLR generally does not affect P concentration in MG-Si. Similarly, Fig. 3(b) shows the variation in the concentration of P during MNPOLR; in general, the concentration of P in MG-Si was decreased relative to that in C-MG-Si. Meanwhile, the calculated average concentration of P in C-MG-Si before MNPOLR was 0.0218 wt.%, and that in MG-Si after MNPOLR was reduced to 0.0155 wt.%. In contrast to COLR, MNPOLR significantly reduced the concentration of P in MG-Si.

To intuitively observe the difference in P separation between two technologies, the relative removal efficiency of P in each batch of materials was determined; the calculation results are shown in Fig. 4. With COLR, the relative removal efficiency of P ranged from −9.2814% to 8.7087%; that in Batches 1-3 was less than 0%, whereas that in

Batches 4 and 5 exceeded 0% but was less than 10%, indicating that P was deposited in MG-Si in general. The average relative removal efficiency of P was −1.9428%, indicating that P was difficult to separate from C-MG-Si during COLR and P was slightly enriched in MG-Si after COLR. After the introduction of an MNP, the relative removal efficiency of P was distributed between −31.6901% and 54.6980%. A negative removal efficiency (−31.6901%) was exhibited only in Batch 3; the relative removal efficiency of P in the other four batches exceeded 20%. In general, the average relative removal efficiency of P reached 21.7638%, which was 23.7066% higher than that under COLR, realizing the breakthrough of P from impossible to effective separation.

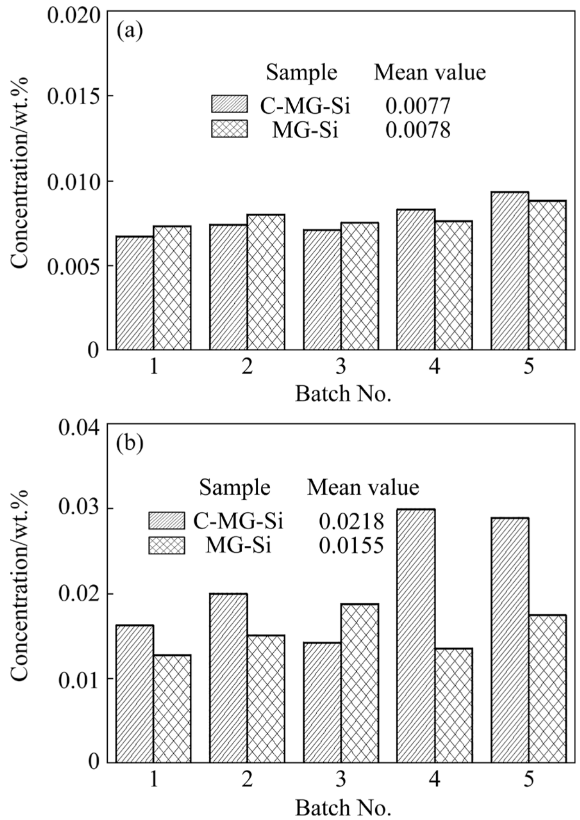

Fig. 3 Effect of oxidative ladle refining on impurity concentration in MG-Si: (a) Conventional oxidative ladle refining; (b) Micro negative-pressure oxidative ladle refining

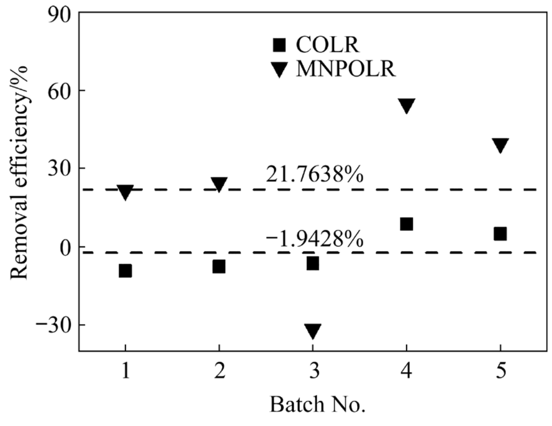

Fig. 4 Effect of micro negative pressure on removal efficiency of P during oxidation ladle refining

3.2 Distribution characteristics of P between slag and MG-Si

In Section 3.1, relative separation efficiency indices of P with COLR and MNPOLR are determined by comparing C-MG-Si with MG-Si. However, in addition to MG-Si, the refining slag is also a major product derived from C-MG-Si after OLR. The distribution coefficient of P between Slag and MG-Si is an important basis for determining the mechanism of P separation. Before the distribution coefficient analysis, the properties of slags produced with the two processes had to be statistically analyzed. LI et al [21] evaluated the effects of different compositions and basicity on the distribution coefficient of P. The result in Eq. (7) shows that an increase in basicity (B) could increase the capacities of P ($C_{PO_4^{3-}}$) in slag, but the separation of P from Si melt was difficult to achieve.

$$\ln C_{PO_4^{3-}}=79.9B+10.9 \tag{7}$$

In the current study, the XRF characterization results revealed that the average concentrations of Al and Ca in the slags produced by COLR and MNPOLR were determined from the experiment. As shown in Table 1, the average concentrations of Al and Ca with COLR and MNPOLR are 5.3800 and 23.9716 wt.%, respectively, and 6.7918 and 21.7164 wt.%, respectively. Owing to a small amount of impurities and inclusion Si retained in slag, the total amount is usually lower than 15 wt.% [22]. Thus, the basicity of the slag (B) produced with the two methods is calculated using Eq. (8), where w is the mass of the corresponding oxide, and ε is the total amount of the Si inclusion and other impurities and its value ranges from 0 to 15 wt.%. The calculation results show (Table 1) that the basicity of the slag produced by COLR ranged from 0.5963 to 0.8130 and that by MNPOLR ranged from 0.5355 to 0.7279. Moreover, the introduction of micro negative pressure reduced the basicity of the slag phase.

$$B=\frac{w_{\mathrm{CaO}}}{w_{\mathrm{SiO_2}}}=\frac{w_{\mathrm{CaO}}}{100-w_{\mathrm{CaO}}-w_{\mathrm{Al_2O_3}}-\varepsilon} \quad (8)$$

Table 1 Average concentrations of Al and Ca and basicity of slag

Sample	Concentration of Al/wt.%	Concentration of Ca/wt.%	Basicity
COLR	5.3800	23.9716	0.5963−0.8130
MNPOLR	6.7918	21.7164	0.5355−0.7279

The calculation results of the distribution coefficients of P between Slag and MG-Si are shown in Fig. 5. The distribution coefficients of P in all MNPOLR samples were smaller than those in COLR samples. The average distribution coefficients of P in the COLR and MNPOLR samples were 0.9529 and 0.0962, respectively. These results indicate that the dissolution of P in the slag was reduced after MNPOLR, and the concentration of P that remained in the MG-Si melt was higher than that in the slag at the equilibrium P concentration between the slag and MG-Si. The distribution behavior of P matched the composition characteristics of the slag. The MNP environment reduced the basicity of slag, leading to a decrease in the dissolved amount of P in the slag, which was consistent with the conclusion of LI et al [21]. However, this outcome did not match the removal efficiency of P, particularly the enhanced separation of P in the MNPOLR sample; the residual amount of P in MG-Si decreased, and the enrichment ratio of P in the slag should be increased theoretically. The distribution coefficient of P in the MNPOLR sample was expected to exceed 1, considering that the slag yield during the production of MG-Si was less than 10% of the MG-Si yield but instead was only 0.0962. Errors in the system were systematically resolved; the only error source identified in the experiment was the fume that could not be collected completely and independently. Therefore, the enhanced removal of P in the MNP environment was mainly attributed to P, together with the fume via the gas phase, with the following considered: the removal efficiency of P in the MNPOLR samples, the composition characteristics of the slag phase, and the distribution results of P between the slag and MG-Si.

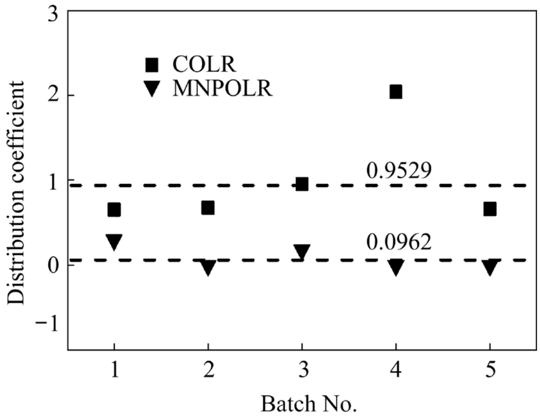

Fig. 5 Effect of oxidative ladle refining on P distribution in slag/MG-Si phase

3.3 Enhanced separation mechanism of P

On the basis of the results and discussion in Sections 3.1 and 3.2, the introduction of an MNP environment promoted the separation of P from MG-Si, and the distribution characteristics of P indicated that P was mainly separated via gas phase transport rather than being enriched in slag. To further determine the enhanced separation mechanism of P in the MNP, the dominant thermodynamic characteristics of P and the kinetic behavior of P separation under OLR conditions were fully discussed. The temperature of oxidative refining typically ranges from 1773 to 2273 K, and the composition of C-MG-Si could be simplified to the Si−Ca−Al−Fe−P five-element system under the assumption that O_2 is sufficient in the system. As shown in Fig. 6, the Gibbs free energy of formation of all types of oxidative products that may be generated by P in the Si−Ca−Al−Fe−P system was calculated by the reaction module in FactSage, under the standard condition of 1 mol P. The Gibbs free energy of all oxidative products of P is less than −100 kJ/mol, indicating that all oxidative products of P can be generated under refining conditions, with $Ca_7P_2Si_2O_{16}$ being the most stable and most likely to be generated.

Owing to a large amount of Si in the refining system, excess Si is always present in the reaction. The calculation standard Gibbs free energy change under the same oxygen standard, which is usually fundamental and ignores the formation of other oxides and the interactions between components in complex systems. As shown in Fig. 7 the stable equilibrium composition of the 90Si−4Ca−3Al−2Fe−1P+20O$_2$ system at temperatures ranging from

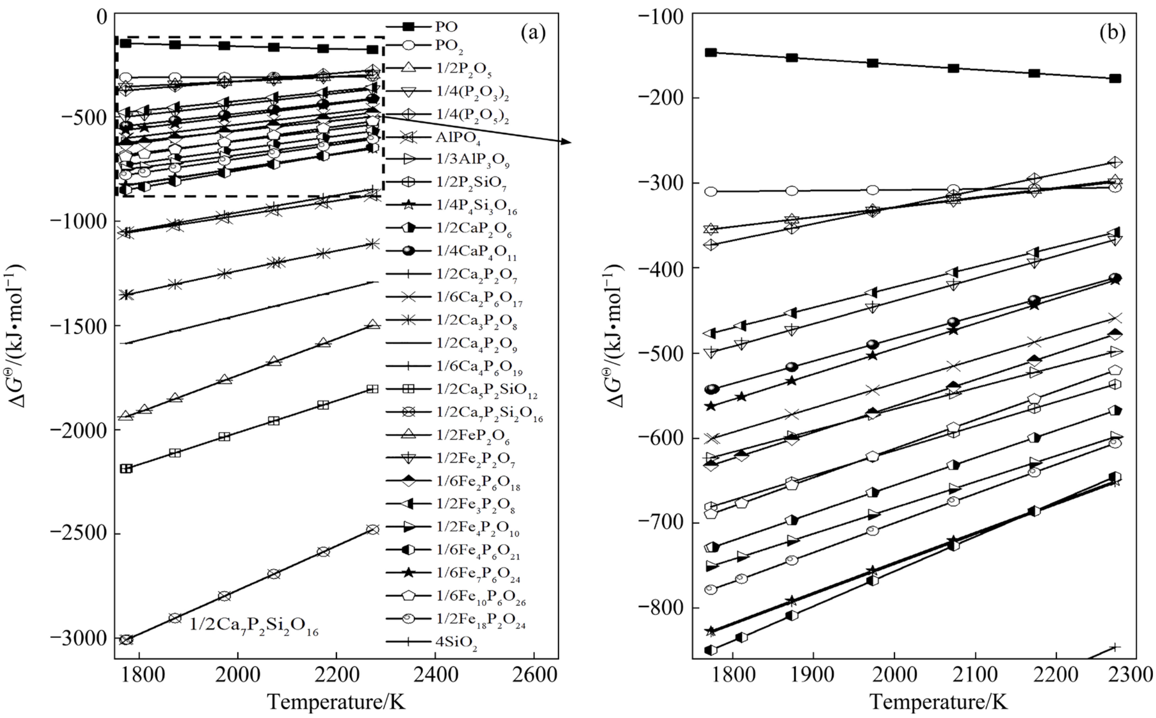

Fig. 6 Gibbs free energy changes of oxidation product of P with oxidative ladle refining

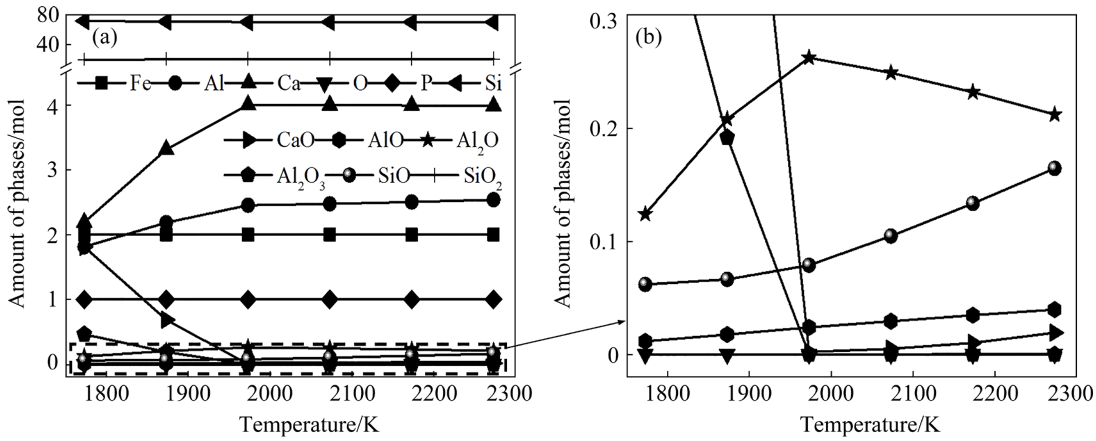

Fig. 7 Equilibrium product composition of oxidation product of P with oxidative ladle refining

1773 to 2273 K was calculated using the equilibrium module in FactSage. When the temperature exceeds 1973 K, Si and Al are mainly oxidized, and SiO_2, SiO, Al_2O, and AlO are generated. Ca is mainly oxidized to CaO in the temperature region below 1973 K. During the process, P is not oxidized and exists in the form of elemental P in the system. This result is primarily attributed to the reducing action produced by excessive Si and the formation of other oxides is preferentially related to P.

During OLR of C-MG-Si, P exists stably as elemental atoms, establishing the basis of the mechanism underlying P volatilization separation. In general, the volatilization separation of P from the melt mainly consists of three steps [23,24]:

(1) P diffuses from the melt to the gas/liquid interface;

(2) P evaporates from the gas/liquid interface into the gas phase;

(3) Diffusion of P in the gas phase.

Blowing refining is the basis of OLR; thus, continuous blowing of gas from the bottom of the lift to the C-MG-Si melt forms turbulent kinetic energy in the melt in the main direction toward the melt surface, inducing strong agitation for the melt [25]. Therefore, as the melt moves toward the surface, the diffusion behavior of P from the melt to the gas/liquid interface is not restricted; that is, the diffusion of P from the melt to the gas/liquid interface does not become the rate control step of P volatilization separation. After P diffuses to the gas/liquid interface, the gasification reaction of P occurs. The specific reaction is affected by conditions such as P activity and temperature. The gasification reaction of P and the Gibbs free energy generated by different gasification products are expressed in Eqs. (9)−(12) [26]. Meanwhile, P has the largest saturated vapor pressure and the lowest boiling point in the C-MG-Si system [27]. Therefore, the thermodynamic conditions for P gasification are sufficient, and P gasification is hardly the main step for controlling the rate of P volatilization separation:

$$P=P(g),\ \frac{1}{2}P_2(g),\ \frac{1}{4}P_4(g) \tag{9}$$

$$\Delta G_{P}^{\Theta}=387000(\pm 2000)-103(\pm 10)T \tag{10}$$

$$\Delta G_{P_2}^{\Theta}=139000(\pm 2000)-43.4(\pm 10.1)T \tag{11}$$

$$\Delta G_{P_4}^{\Theta}=81625-4.8T-0.0008T^2 \tag{12}$$

After partial gasification, while the gas/liquid equilibrium of P is formed at the gas/liquid interface, P separated from the gas/liquid interface is rapidly oxidized because of the absence of the reduction effect of Si. During gas phase diffusion above the melt, both the elemental P and P oxide are subjected to upward flotage and downward resistance, which are mainly caused by a molecular collision in the gas phase. Supposing that P (with quantity of N) evaporates at the gas/liquid interface, when they enter the gas phase and diffuse the dl distance, they are affected by the gas phase resistance and collide with molecules in the gas phase, reducing dN P. The mean free path (λ) of the vaporized P can be determined using Eq. (13). The lower the gas phase resistance, the smaller the value of dN, and more P is separated by gas-phase diffusion. On the basis of the aforementioned discussion, the transformation from COLR to MNPOLR results in the enhanced separation of P. The mechanism is shown in Fig. 8.

$$\lambda=\frac{N\cdot \mathrm{d}l}{-\mathrm{d}N} \tag{13}$$

During COLR, P is transferred to the gas/liquid interface by melt agitation, and part of the oxidized P is captured by the slag. However, owing to the presence of a large number of Si systems, the oxides of P are eventually reduced to the form of elemental atoms and then returned to the Si melt; a small number remains in the slag phase. Simultaneously, the other part of P at the gas/liquid interface is vaporized; however, owing to the retention of a large amount of fume above the melt, P collides with the fume molecules during gas phase diffusion. This part of P is subjected to large diffusion resistance; only a small amount of P can escape successfully, and the part that returns to the

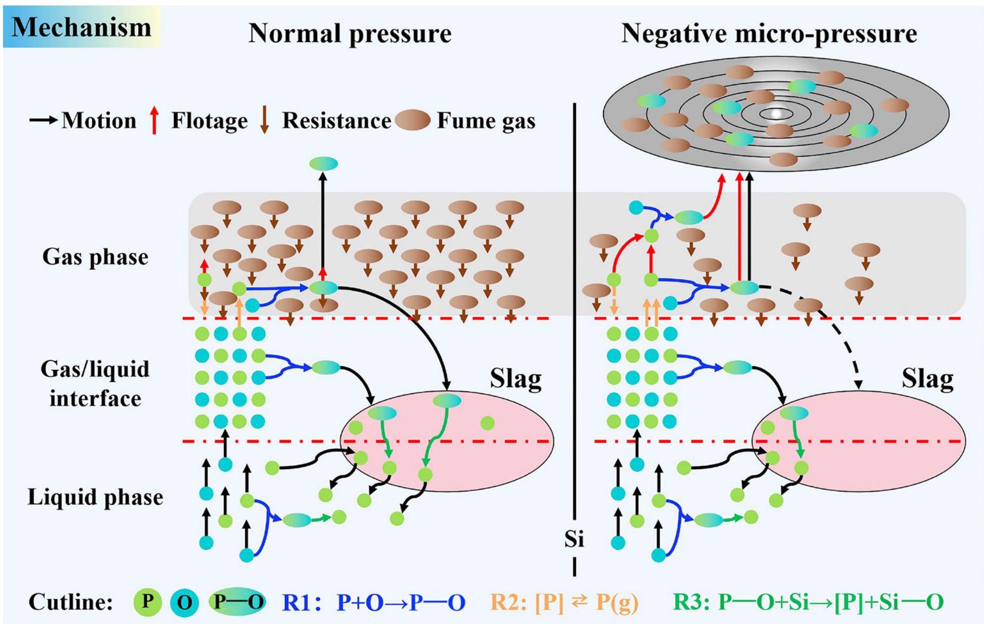

Fig. 8 Mechanism of enhanced P separation by micro negative pressure

melt, is captured by the slag, and eventually returns to MG-Si. Therefore, with the COLR method, P is difficult to oxidize, and its gas phase volatilization efficiency is extremely low, ultimately impeding the effective separation of P. With the MNPOLR approach, MNP separates the fume from the top of the melt, lowers the resistance of the gas phase, and provides enhanced buoyancy, thus promoting P transport in the gas phase and strengthening the evaporation separation of P. During the process, the basicity of the slag phase decreases, and the capacity of P in the slag phase is reduced, thereby enhancing P entry to the gas phase.

4 Conclusions

(1) Comparison of the removal efficiency of P with the COLR and MNPOLR methods showed that the introduction of an MNP environment increased the average relative removal efficiency of P from −1.9428% to 21.7638%, realizing efficient separation of P during OLR.

(2) After MNP was introduced, the basicity of the slag produced by OLR decreased, and the distribution coefficient of P between the slag and MG-Si decreased from 0.9529 to 0.0962. P in the refining slag strengthened by MNPOLR separation was not enriched but entered the fume phase.

(3) The calculation of the reaction module and the equilibrium module by using FactSage showed that P in the Si−Ca−Al−Fe−P system could not exist stably in an oxide form but always remained in elemental P form at refining temperatures ranging from 1773 to 2273 K. Despite the low boiling point and high saturated vapor pressure of P, the volatilization of P was controlled by diffusion in the gas phase because of the high resistance of the retained fume under the COLR technique. The introduction of MNP reduced the gas phase resistance above the melting point, facilitated the gas phase diffusion of P, and realized the enhanced separation of P in gas-phase transport.

Acknowledgments

The authors are grateful for the financial supports from the National Natural Science Foundation of China (No. U1902219), the Yunnan Young and Middle-aged Academic and Technical Leader Reserve Talent Project, China (No. 2018HB009), the Yunnan Outstanding Youth Science Foundation, China (No. 202101AV070007), and the Major Science and Technology Projects in Yunnan Province, China (Nos. 2019ZE007, 202002AB080002)

References

[1] WODITSCH P, KOCH W. Solar grade silicon feedstock supply for PV industry [J]. Solar Energy Materials and Solar Cells, 2002, 72: 11−26.

[2] GILLOT B, WEBER G, SOUHA H, ZENKOUAR M. Reactivity of commercial silicon and silicides towards copper(I) chloride: Effect of aluminium, calcium and iron on the formation of copper silicide [J]. Journal of Alloys and Compounds, 1998, 270: 275−280.

[3] WU Ji-jun, MA Wen-hui, LI Yan-long, YANG Bin, LIU Da-chun, DAI Yong-nian. Thermodynamic behavior and morphology of impurities in metallurgical grade silicon in process of O_2 blowing [J]. Transactions of Nonferrous Metals Society of China, 2013, 23: 260−265.

[4] LU Hai-fei, WEI Kui-xian, MA Wen-hui, XIE Ke-qiang, WU Ji-jun, LEI Yun. The effect of secondary refining on the removal of phosphorus from metallurgical-grade silicon by acid leaching [J]. Metallurgical & Materials Transactions B, 2017, 48: 2768−2780.

[5] WANG Xin-guo, DING Wei-zhong, TANG Kai, JIANG Guo-chang, XU Kuang-di. Experimental thermodynamic research on equilibrium between silicon alloy and SiO_2−CaO−Al_2O_3 melt [J]. Transactions of Nonferrous Metals Society of China, 2001, 11: 535−539.

[6] HE Nai-yong, YANG Ding, XU Min, WU Ji-jun, MA Wen-hui. Oxidation kinetics of impurities in metallurgical-grade silicon melt by O_2 blowing refining process [J]. Metallurgical and Materials Transactions B, 2021, 52: 1830−1838.

[7] BJØRNSTAD E L, TRANELL G M. Nucleation of SiO_2−CaO−Al_2O_3 slag in oxidative ladle refining of metallurgical grade silicon [J]. Metallurgical and Materials Transactions B, 2021, 52: 1392−1412.

[8] KERO I, MARI K N, ANDERSEN V, TRANELL G M. Refining kinetics of selected elements in the industrial silicon process [J]. Metallurgical and Materials Transactions B, 2015, 46: 1186−1194.

[9] WU Ji-jun, MA Wen-hui, YANG Bin, DAI Yong-nian, MORITA K. Boron removal from metallurgical grade silicon by oxidizing refining [J]. Transactions of Nonferrous Metals Society of China, 2009, 19: 463−467.

[10] SUN Jin-ling, JIE Jin-chuan, ZOU Qing-chuan, GUO Li-juan, CAO Zhi-qiang, WANG Tong-min, LI Ting-ju. Boron removal from molten silicon using CaO−SiO_2−BaO−CaF_2 slag [J]. Transactions of Nonferrous Metals Society of China, 2016, 26: 3299−3304.

[11] SAFARIAN J, TANGSTAD M. Vacuum Refining of molten silicon [J]. Metallurgical and Materials Transactions B, 2012, 43: 1427−1445.

[12] ZHU Meng-yi, YUE Sheng-ying, WU Gui-xuan, TANG Kai,

XU Yi-jiang, SAFARIAN J. P removal from Si by Si−Ca−Al alloying-leaching refining: Effect of Al and the $CaAl_2Si_2$ phase [J]. Separation and Purification Technology, 2021, 271: 118675.

[13] ZHANG Cong, WEI Kui-xian, ZHENG Da-min, MA Wen-hui, DAI Yong-nian. Phosphorus removal from upgraded metallurgical-grade silicon by vacuum directional solidification [J]. Vacuum, 2017, 146: 159−163.

[14] XI Feng-shuo, LI Shao-yuan, MA Wen-hui, CHEN Zheng-jie, WEI Kui-xian, WU Ji-jun. A review of hydrometallurgy techniques for the removal of impurities from metallurgical-grade silicon [J]. Hydrometallurgy, 2021, 201: 105553.

[15] XIA Zhen-fei, WU Ji-jun, MA Wen-hui, LEI Yun, WEI Kui-xian, DAI Yong-nian. Separation of boron from metallurgical grade silicon by a synthetic $CaO-CaCl_2$ slag treatment and $Ar-H_2O-O_2$ gas blowing refining technique [J]. Separation and Purification Technology, 2017, 187: 25−33.

[16] XU Min, ZHU Yun-yang, WU Ji-jun, XIA Zhen-fei, MA Wen-hui. Mechanism of boron removal using calcium silicate slag containing $CaCl_2$ under O_2 atmosphere [J]. Metallurgical and Materials Transactions B, 2021, 52: 2573−2581.

[17] LI Jing-wei, BAI Xiao-long, BAN Bo-yuan, HE Qiu-xiang, CHEN Jian. Mechanism of boron removal from Si−Al melt by $Ar-H_2$ gas mixtures [J]. Transactions of Nonferrous Metals Society of China, 2016, 26: 3046−3051.

[18] WANG Zhi, GE Zhi, LIU Junhao, QIAN Guoyu, DU Bing. The mechanism of boron removal from silicon alloy by electric field using slag treatment [J]. Separation and Purification Technology, 2018, 199: 134−139.

[19] DENG Xiao-cong, LI Sheng, WEN Jian-hua, WEI Kui-xian, ZHANG Ming-yu, YANG Xi, MA Wen-hui. Mechanism of enhancing phosphorus removal from metallurgical grade silicon by Si−Fe−Ti phase reconstruction [J]. Metallurgical and Materials Transactions B, 2021, 52: 625−632.

[20] LEI Yun, MA Wen-hui, WU Ji-jun, WEI Kui-xian, LI Shao-yuan, MORITA K. Impurity phases and their removal in Si purification with Al−Si alloy using transition metals as additives [J]. Journal of Alloys and Compounds, 2018, 734: 250−257.

[21] LI M, UTIGARD T, BARATI M. Removal of boron and phosphorus from silicon using $CaO-SiO_2-Na_2O-Al_2O_3$ flux [J]. Metallurgical and Materials Transactions B, 2014, 45: 221−228.

[22] TAN Ning, LI Hao, DING Zhao, WEI Kui-xian, MA Wen-hui, WU Dan-dan, HAN Shi-feng. Hydrogen generation during the purification of metallurgical-grade silicon [J]. International Journal of Hydrogen Energy, 2020, 45: 23406−23416.

[23] SHI Shuang, DONG Wei, PENG Xu, JIANG Da-chuan, TAN Yi. Evaporation and removal mechanism of phosphorus from the surface of silicon melt during electron beam melting [J]. Applied Surface Science, 2013, 266: 344−349.

[24] TAN Yi, GUO Xiao-liang, SHI Shuang, DONG Wei, JIANG Da-chuan. Study on the removal process of phosphorus from silicon by electron beam melting [J]. Vacuum, 2013, 93: 65−70.

[25] WANG Jie, CHEN Zheng-jie, MA Wen-hui, WEI Kui-xian, LI Shao-yuan, LIU Jun-ru, DING Wei-min, WEN Jian-hua. Effect of off-centered silicon ladle on the removal strength of aluminum and calcium impurities [J]. Separation and Purification Technology, 2018, 201: 301−308.

[26] ZHENG Song-sheng, ENGH T A, TANGSTAD M, LUO Xue-tao. Separation of Phosphorus from silicon by induction vacuum refining [J]. Separation and Purification Technology, 2011, 82: 128−137.

[27] ZHENG Song-sheng, SAFARIAN J, SEOK S, SUNGWOOK K, TANGSTAD M, LUO Xue-tao. Elimination of phosphorus vaporizing from molten silicon at finite reduced pressure [J]. Transactions of Nonferrous Metals Society of China, 2011, 21: 697−702.

在氧化抬包精炼过程引入微负压实现磷从冶金级硅中的分离

邓小聪[1,2]，魏奎先[1,2,3]，马文会[1,2,3]，唐绮唯[1,2]，张 辉[1,2]

1. 昆明理工大学 冶金与能源工程学院，昆明 650093；

2. 昆明理工大学 真空冶金国家工程实验室，昆明 650093；

3. 昆明理工大学 省部共建有色金属资源清洁利用国家重点实验室，昆明 650093

摘 要：通过在氧化抬包精炼过程中引入微负压(MNP)环境实现 P 从冶金级硅(MG-Si)中的稳定分离。引入 MNP 环境后，P 的相对去除效率从−1.9428%增长至 21.7638%。在微负压氧化抬包精炼(MNPOLR)过程中，P 没有被富集在渣中而是通过气相传输被强化分离。尽管 P 具有低沸点和高饱和蒸气压的特点，但在传统氧化抬包精炼过程中 P 的挥发受到气相扩散控制。MNPOLR 可以持续分离熔体上方烟气进而削弱 P 的气相扩散阻力，促进 P 从 MG-Si 中的分离。因此，MNPOLR 是一种有效且可被推广的除 P 技术。

关键词：氧化抬包精炼；微负压；分离；磷；冶金级硅

(Edited by Bing YANG)